

Food-grade titanium dioxide induces toxicity in *C. elegans* and acute hepatic and pulmonary response in mice

Giovanni Sitia^{1^}, Fabio Fiordaliso^{2^}, Martina B Violatto², Jennifer Fernandez Alarcon², Laura Talamini², Alessandro Corbelli², Lorena Maria Ferreira¹, Ngoc Lan Tran¹, Indranath Chakraborty³, Mario Salmona², Wolfgang J. Parak³, Luisa Diomede^{2*} and Paolo Bigini^{2*}

¹ Experimental Hepatology Unit, Division of Immunology, Transplantation and Infectious Diseases, IRCCS San Raffaele Scientific Institute, Via Olgettina 58, 20132 Milano, Italy.

² Department of Molecular Biochemistry and Pharmacology, Istituto di Ricerche Farmacologiche Mario Negri IRCCS, Via Mario Negri 2, 20156 Milano, Italy.

³ Center for Hybrid Nanostructures (CHyN), Universität Hamburg, Luruper Chaussee 149, 22607 Hamburg, Germany.

[^] S.G. and F.F. contributed equally to this work.

* Correspondence: Luisa Diomede, luisa.diomede@marionegri.it; Paolo Bigini, paolo.bigini@marionegri.it

Abstract: Food-grade titanium dioxide (E171) contains variable percentages of TiO₂ nanoparticles (NPs) posing awareness about its potential effects on human and animal health. Despite many studies, the actual relationship between the physicochemical properties of E171 NPs and their interaction with biological targets is still far from clear. We evaluated the acute toxicity of E171 in invertebrate and vertebrate animals. In the nematode *C. elegans*, E171 up to 1.0 mg/mL did not affect worm's viability and lifespan but significantly impaired pharyngeal function, reproduction, and development. We also focused our attention on the fate of E171 after its penetration inside the circulatory tree, investigating whether its intravenous administration to mice could result in an acute over-absorption to filter organs. A significant increase of hepatic Ti concentration and the formation of microgranulomas were observed. Interstitial inflammation and parenchymal modification were found in lung coupled with Ti accumulation, probably due to the propensity of TiO₂NPs to agglomerate, as demonstrated by transmission electron microscopy experiments showing that the incubation of E171 with serum promoted the formation of compact clusters. Overall, these data emphasize, once again, the actual risk for human and animal exposure to E171.

Keywords: Titanium dioxide; E171; *C. elegans*; mice; toxicity

1. Introduction

Understanding the biological interactions between nanoparticles (NPs) generated in large-scale production processes and biological matrices (cells, tissues and whole organism) is a priority for defining their impact on human and environmental health (Chow et al., 2006). Particular concern is aroused by the evidence of potential effects of NPs of different origin and chemical composition stimulating the production of radical oxygen species (ROS) and activating an inflammatory response in peripheral organs of the digestive and respiratory systems (Pope et al., 2004) (Tucci et al., 2013) (Trouiller et al., 2009).

Out of the wide range of nanomaterials produced on purpose or unintentionally in industrial processes, titanium dioxide (TiO₂) is the most widely used in the world for a wide range of applications, with 3000 tons produced each year (Musial et al., 2020) (Titanium dioxide market trends analysis report, 2021-2028.). TiO₂ is chemically stable and very hard to dissolve in aqueous solutions (Kakihana et al., 2010). Its exposure in workplaces raises significant questions about occupational risks for workers because, as stated by the International Agency for Research on Cancer (IARC) (IARC, 1997), TiO₂ bulk material is a possible carcinogen for humans if inhaled and is classified as 2B (Riebeling et al., 2020).

Occupational exposure to applied TiO₂, typically nanosized, is regulated by two additional regulatory guidelines from the USA National Institute for Occupational Safety and Health (NIOSH) and from the expert panels of the Japanese New Energy and Industrial Technology Development Organization (NEDO). The inertness and persistence of

TiO₂ NPs in the body might be a critical issue in terms of safety and large-scale production plans, for that reason, closer attention must be paid to its exposure.

On account of their physicochemical properties TiO₂ NPs are used for a variety of applications, such as manufacture of high refractive index products (e.g., coatings, plastics, paints), photocatalysts (water treatment and air purification), products such as sunscreens and toothpaste (Titanium dioxide market trends analysis report, 2021-2028) (Scientific Committee on Consumer Safety SCCS OPINION on Titanium dioxide (TiO₂), and cosmetics that lead to exposure by inhalation) (CFR - Code of Federal Regulations Title 21) (EFSA, 2016). In nature, primarily TiO₂ occurs in the form of the minerals brookite, rutile and anatase. However, only rutile and anatase can be used without surface treatment and coating as the food additive E171 (EFSA, 2021) (EFSA, 2016). E171 consists of particles typically ranging from 20-300 nm in diameter (EFSA, 2016) and the percentage of NPs with a diameter of <100 nm ranges from 10% up to 45% depending on their manufacturing conditions (Weir et al., 2012) (Peters et al., 2014) (Dudefoi et al., 2017) (Fiordaliso et al., 2018). According to the European Union Regulations 2011/696/EU (ISO/TS 80004-1:2015) (ISO/TS 80004-2:2015), E171 cannot be considered a nanomaterial because the proportion of NPs with one or more external dimensions in the size range below 100 nm is less than 50%. However, the wide use of E171 in products ingested daily by millions of consumers and its possible dispersion into the environment have raised awareness of its potential side effects on human and animal health (Fiordaliso et al., 2022).

Once ingested, TiO₂ NPs can cross biological membranes, enter cells, and accumulate in tissues and organs where they exert toxicity and can trigger both local and systemic responses (Shi et al., 2013). E171 can enter the bloodstream, accumulate in the digestive organs and affect gastrointestinal function. It can also accumulate in the reproductive system, pass through the placenta, and be transferred from the maternal to fetal circulation (Shi et al., 2013) (Zhang et al., 2012) (Guillard et al., 2020) (E Rollerova et al., 2015).

Despite a large number of studies, the actual relationship between the physicochemical properties of food-grade TiO₂ NPs and their interaction with biological targets is still far from clear. Although the results of *in silico* and *in vitro* analyses are absolutely necessary to have a first idea of the potential toxicity of NPs, depending on their geometry or surface charge, they are rarely transferable to multicellular organisms. The recent decision taken from EU, to ban E171 as food additive (EFSA, 2021) furthermore strengthens the potential risks, including the acute toxicity, related to its over-exposure. Thus, testing the toxicity of E171 in cells up to vertebrates at increasing levels of biological complexity is urgently needed.

In the present study we evaluate the acute toxicity of E171 in two different animal models. We first evaluate the effect of E171 in the invertebrate nematode *C. elegans* already employed to test the effects of TiO₂ NPs of various shapes and sizes (Iannarelli et al., 2016) (Ma et al., 2019) (Hu et al., 2020). Rod-shaped TiO₂ NPs were more toxic for worms than bipyramidal and spherical ones and severely affected the pharyngeal function, reproduction, and larval growth, although no difference in biological distribution and accumulation was found (Iannarelli et al., 2016). E171, at doses which did not affect worm's viability and lifespan, significantly impaired pharyngeal function, reproduction, and development. It is important to note that toxicity data on worms provide information from a whole animal with intact and metabolically active digestive, reproductive, endocrine, sensory, and neuromuscular systems and, importantly similar toxic modes of action have been noted in *C. elegans* and mammals (Hunt, 2017). This nematode is thus a reliable model for human pathophysiology. *C. elegans* was selected not only for its well-conserved signal pathways and high level of gene homology with humans, but also to obtain useful information on the toxicity of E171 for environmental health, particularly for terrestrial and aquatic animals. This nematode is in fact ubiquitous worldwide and can live in soil and water (Frézal and Félix, 2015).

We recently investigated that repeated oral administration of E171 to mice, at a dose level comparable to estimated human dietary exposure, resulted in Ti deposition in the digestive system and a massive intestinal adsorption, bloodstream circulation and

inflammatory action to the liver (Talamini et al., 2019). In the present study, we focused our attention on the fate of E171 after its penetration inside the circulatory tree mimicking an accidental overloading in humans. We decided to make a single intravenous administration at a dose of 6 mg/kg body weight (b.w) to mimic the potential risk due to a massive overexposure to E171 ingestion, the passage in the circulation and the penetration in the main filter organs such as liver and lungs. To avoid any possible confounding factor due to upstream sources of stress (e.g. cytokine activation due to gastrointestinal injury) we directly injected E171 in the tail vein of young healthy immunocompetent mice. This is also interesting because of, in spite of a robust body of evidence related to the effect of systemic administration TiO₂ NPs (Bischoff et al., 2021) the impact of E171 in filter organs is poorly documented. Moreover, to determine whether serum affects the colloidal stability of E171 inducing possible structural modifications and/or formation of aggregates, transmission electron microscopy (TEM) analysis was performed. This control is crucial to correlate the behavior of the E171 particles in the biological fluids to their physical and chemical state. We studied the biodistribution of E171 in different organs at different time-points after administration (from 1 hour up to one week) and evaluated some biochemical and histological parameters indicative of alterations related to the toxic profile of E171.

The results achieved indicated that E171 can accumulate in the liver of treated mice where the formation of microgranulomas was caused. A progressive accumulation was also found in the lungs and was accompanied by a massive recruitment of monocytes, macrophage hypertrophy and focal parenchymal lesion in the alveoli, these data gave us an interesting overview on the impact of E171 for human and animals health.

2. Materials and Methods

2.1. *C. elegans* studies

The *C. elegans* strain Bristol N2, obtained from the *Caenorhabditis elegans* Genetic Center (CGC; University of Minnesota), was propagated at 20°C on solid nematode growth medium (NGM) seeded with *Escherichia coli* OP50 (from CGC) as food. The effect of E171 on worm mortality, pharyngeal function, reproduction, and development was investigated as described by Iannarelli et al. (Iannarelli et al., 2016).

To determine the effect on pharyngeal function, age-synchronized nematodes (L4 larval stage) were collected with M9 buffer, centrifuged, and washed twice with 5 mM phosphate-buffered saline (PBS), pH 7.4, to remove bacteria. Worms were suspended in water and incubated with freshly suspended E171 in water at a concentration of 0.01-1.0 mg/mL (100 worms/100 µL) without *E. coli*, to avoid potential interference between bacteria and the nanomaterial. Control worms were incubated with water only (100 worms/100 µL). After 2 hours, the worms were transferred to NGM plates seeded with OP50 *E. coli*. Mortality was recorded 2 and 24 hours after treatment by counting the paralyzed worms. At the same times, pharyngeal pumping efficiency was measured by counting the number of times the terminal bulb of the pharynx contracted in a 1min interval (pumps/min).

Age-synchronized L4 nematodes were used to determine the effect of E171 on reproduction and larval development. Worms were incubated for 2 hours without *E. coli*, with freshly suspended E171 in water alone 0.1-0.5 mg/mL (100 worms/100 µL). Control worms were incubated with water (vehicle). *C. elegans* were transferred to NGM plates seeded with fresh OP50 *E. coli*, and the eggs laid were counted after 6h incubation at 20°C. The adults were then removed and the plates were stored at 20°C. The worms in the different larval stages (L1, L2, L3, L4 and adult) were counted 16, 24, 36 and 48 hours after eggs hatched.

For lifespan experiments, worms at larval stage L3 were fed for 2 hours with 0.2 mg/mL E171 freshly suspended in water (100 worms/100 µL) or water alone (vehicle). Nematodes were then transferred to fresh NGM plates seeded with *E. coli*. To avoid overlapping generations, worms were transferred to fresh NGM plates seeded with *E. coli* every day until they stopped laying eggs. The live worms were counted each consecutive day until all worms were dead, and the number of live worms was scored.

2.2. Transmission electron microscopy (TEM)

Food-grade TiO₂ (E171, Pretiox AV01PhG), kindly provided by Giusto Faravelli S.p.A. (Milan, Italy), was a 99.3% pure TiO₂ anatase product complying with the standard regulations of the European and US Pharmacopoeia, Food and Drug Administration (FDA) and Food Additive Regulations. The physico-chemical characteristics of this material have been already deeply characterized in our previous works by single particle inductively coupled plasma-mass spectrometry (ICP-MS), dynamic laser light scattering (DLS), Nanoparticle Tracking Analysis (NTA) and TEM (Fiordaliso et al., 2018) (Talamini et al., 2019). To study whether serum could over time affect the morphology and colloidal properties of E171, TEM analysis was performed incubating 1 mg/100 µL of E171 in H₂O or murine serum for 1, 4 and 24 hours. The samples were not sonicated to avoid any effects on the particle characteristics that would not occur in realistic conditions of use and 5 µL of each sample were placed into a formvar/carbon-coated copper grid (100 mesh) (Electron Microscopy Sciences, Washington, PA, USA) and air-dried at room temperature. NP images were obtained with an Energy Filter Transmission Electron Microscope (EFTEM, ZEISS LIBRA® 120) coupled with an yttrium aluminum garnet (YAG) scintillator slow-scan CCD camera (Sharp eye, TRS, Moorenweis, Germany), with a Focus Aid option, enabling us to reach the precise eucentric plane in the observation of each single NP (Fiordaliso et al., 2018).

2.3. Mouse studies

The Mario Negri Institute for Pharmacological Research IRCCS adheres to the principles set forth in the following laws, regulations and directives concerning the care and use of laboratory animals: Italian Law (D.lgs 26/2014; Authorization No. 19/2008-A issued on March 6, 2008 by the Ministry of Health); Mario Negri Institutional Regulations and Policies, which provide for internal authorization for persons conducting animal experiments (Quality Management System Certificate, UNI EN ISO 9001:2015, Reg. No. 6121); the NIH Guide for the Care and Use of Laboratory Animals (2011 edition); and EU Directives and Guidelines (EEC Council Directive 2010/63/UE). This work was reviewed by the IRCCS-IRFMN Animal Care and Use Committee (IACUC) and subsequently approved by the Italian "Istituto Superiore di Sanità". (Code: 42/2016- PR).

Eight-week-old male CD1 mice (Charles River, Italy) were housed in specific pathogen-free animal rooms at a constant temperature of 21 ± 1°C, humidity 55 ± 10%, a 12h light-dark cycle and free access to food and water. Mice were randomly divided into two groups (9/group). One group was injected intravenously with 6 mg/kg b.w. of E171 suspended in 200 µL of injection grade distilled water. The control group received 200 µL of injection-grade distilled water (vehicle). At selected times (before injection and 1, 12, 24, 96, and 168 hours after), mice were anesthetized with 5% isoflurane, and blood was collected in heparinized tubes from the retro-orbital plexus for analysis, as described previously (Catarinella et al., 2016). Blood from vehicle-treated mice was also used to prepare serum to check the colloidal stability of E171 by TEM. Then, 1, 24, and 168 hours after E171, mice were euthanized and their liver, kidney, spleen, brain, and lungs were collected (3 animals per time point), cleaned with ultrapure water, then subsamples were collected for the determination of TiO₂ content by inductively coupled plasma-mass spectrometry (ICP-MS) and histological examination was done on livers and lungs.

2.4. Biodistribution of TiO₂

TiO₂ was measured in the explanted liver, spleen, kidneys, lungs, brain and blood and quantified using ICP-MS (Agilent 7700 series) (Kreyling et al., 2015). The mouse samples were first digested by the addition of 3 mL of ultra-pure HNO₃ (67% wt) (Fisher Chemical), under constant agitation in 50 mL Falcon tubes for 72h at 22°C till the solution becomes clear and no organics are left in the tube. From the mixture, 100µL were taken and further digested with 100µL of HF acid for 48h to ensure the atomic incidence of the

former TiO₂ NPs. The Ti concentration given by ICP-MS in the original HNO₃ solution of is $C_{Ti} = C'_{Ti} \cdot \alpha_{dil}$ (C' is the actual ICP-MS reading and α_{dil} is the dilution factor). The total mass of Ti in each organ is $m_{Ti} [g] = C_{Ti} \cdot V_{HNO_3}$. We calculated the %ID as m_{Ti} (in each organ) / M_{Ti} (injected Ti mass) *100.

2.5. Blood analysis

Complete blood cell counts were taken in fresh whole blood collected in EDTA-coated microvettes (Sarstedt, Germany) using an automated cell counter (IDEXX Procyte Dx, IDEXX Laboratories). The extent of hepatocellular injury and whole-body toxicity was recorded by measuring serum alanine aminotransferase (sALT), serum aspartate aminotransferase (sAST), and lactate dehydrogenase (LDH) activity. A kinetic UV method optimized by the International Federation of Clinical Chemistry and Laboratory Medicine was used in an Aries chemical analyzer (Werfen Instrumentation Laboratory S.p.A., Italy), and values were expressed as Units/Liter (U/L). Each analysis was validated by a certified biochemical chemistry and hematology specialist using quality control blood (CQI) in the San Raffaele Mouse Clinic (<http://research.hsr.it/en/services/mouse-clinic/hematologic-testing.html>).

2.6. Histopathology

Organs were harvested, fixed in zinc formalin, processed, embedded in paraffin, sectioned, and stained with hematoxylin/eosin (H&E) or further processed for immunohistochemical analysis as previously described (Catarinella et al., 2016). Immunohistochemical staining for tissue-resident monocytes/macrophages was done with the anti-F4/80 specific antibody (clone A3-1, AbD Serotec). All images were acquired using the Aperio Scanscope CS2 system (Leica Biosystems) available at the San Raffaele Advanced Light and Electron Microscopy BioImaging Center (ALEMBIC). Images were identified as representative areas of interest within the total area of the specimen analyzed and exported as ImageScope snapshots.

2.7. Statistical analysis

Data were analyzed using GraphPad Prism 8.0 software. Differences between data groups were analyzed as follows. An independent Student t-test was used for larval growth and F4/80 quantification in lungs. One-way ANOVA followed by Bonferroni *post hoc* test was used for the effect on pharyngeal pumping rate, number of eggs laid in *C. elegans* studies, and Ti accumulation measured by ICP-MS. Two-way ANOVA followed by Bonferroni *post hoc* test was done in serum markers for toxicity (ALT, AST, LDH). The Gehan-Breslow-Wilcoxon test was used for the survival rate of *C. elegans* and a two-tailed Mann-Whitney test for blood cell counts. P values <0.05 were considered statistically significant and reported on graphs. Data are presented as mean \pm standard deviation (S.D.) or mean \pm standard error of the mean (S.E.M.) and depicted in each figure legend.

3. Results

3.1. Toxicity of E171 in *C. elegans*

The toxicity of E171 in *C. elegans* was evaluated analyzing different behavioral endpoints (Fig. 1A-G). Worms were given E171 at subtoxic doses (0.01-1 mg/mL) that did not cause any significant increase in mortality after, 2 or 24 hours (data not shown). In this concentration range there was dose-dependent inhibition of the nematodes' pharyngeal function 2 hours after feeding, with a 50% inhibitory concentration (IC₅₀) of 0.221 ± 0.10 mg/L (Fig. 1B). Pharyngeal inhibition was still comparable 24 hours after feeding (IC₅₀ = 0.211 ± 0.10 mg/mL), indicating that E171 caused a lasting change in feeding (Fig. 1C). The effect reached the plateau already at 0.5 mg/L E171, which caused 76.5% and 82.2% reductions in pharyngeal function, respectively 2 hours and 24 hours after treatment.

The effect of 0.1-0.5 mg/L E171 on the ability of adult worms to reproduce was investigated by counting the eggs laid (Fig. 1D). E171 up to 0.3 mg/L did not affect egg laying, but there was a significant reduction of the reproductive capacity, of respectively 56% and 73%, was observed at 0.4 and 0.5 mg/L. E171 0.2 mg/L modified the larval growth of worms causing a significant increase in the speed of development compared to vehicle (Fig. 1E, F). Thirty-six hours after eggs hatched, E171-fed worms had a higher percentage of worms in L4 ($91.7 \pm 8.3\%$) than vehicle-fed worms ($57.15 \pm 6.2\%$), resulting in a much higher percentage of adult worms 12 hours later. We also examined whether 0.2 mg/L E171 affected worm survival. Median survival was not significantly altered by E171 it was 14 days for vehicle-fed worms and 12 days for E171-fed nematodes (Fig. 1G).

These findings indicate that E171, at doses that did not modify the viability or the lifespan of *C. elegans*, can instead affect their health, with the onset of sub-toxic phenotypes such as impairment in feeding behavior and normal development.

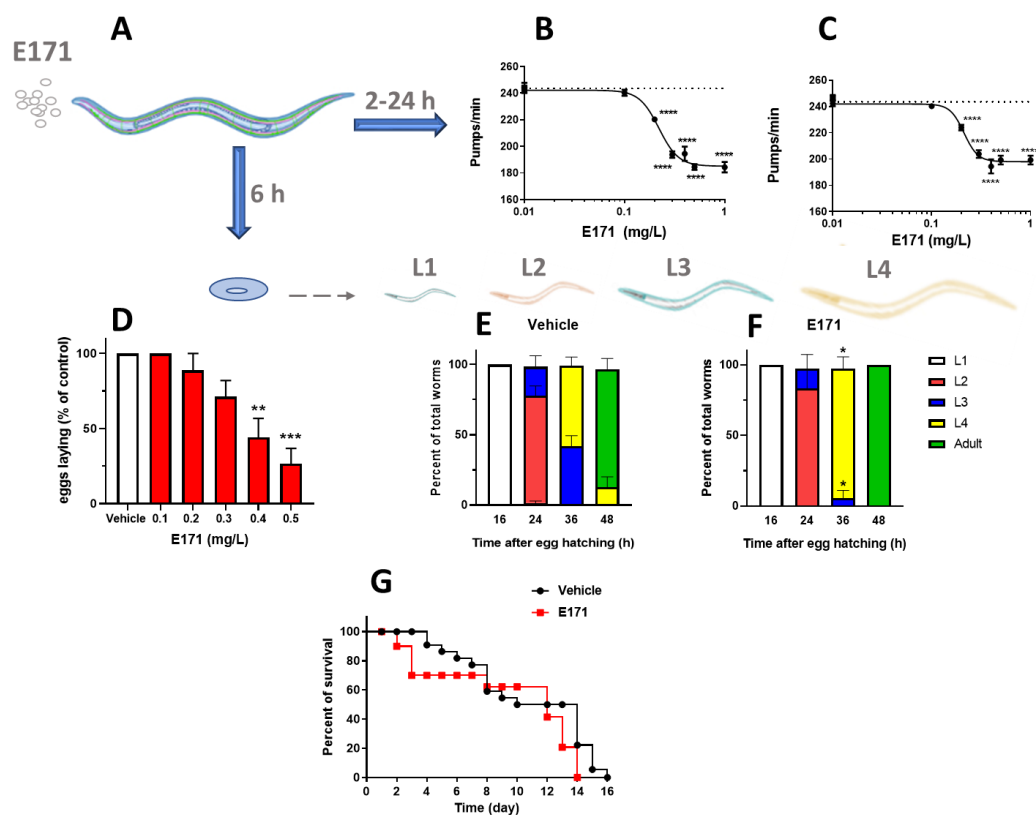


Figure 1. Effects of E171 in *C. elegans*. (A) Worms (100 worms/100 μ L) were fed for 2 hours with E171 freshly suspended in water in the absence of OP50 *E. coli*, then plated on NGM plates seeded with the bacteria and behavioural studies were done different times after plating. Control worms were fed water alone. (B-C) The effect of 0.01-1 mg/L E171 on the pharyngeal pumping rate was scored (B) 2 hours and (C) 24 hours after plating (vehicle, dotted line). Data are the mean \pm SEM (30 worms per group). **** p <0.01 vs vehicle according to one-way ANOVA and Bonferroni *post hoc* test.

(D) The number of eggs laid 6h after plating was expressed as a percentage of the eggs laid by vehicle-fed worms. Mean \pm SEM (10 worms per group). ** $p < 0.005$ and *** $p < 0.0005$ vs vehicle, according to one-way ANOVA and Bonferroni *post hoc* tests. (E, F) Larval growth was rated 16, 24, 36 and 48 hours after eggs hatched, by counting the worms at different larval stages. Data are percentages of the total worms \pm SEM. * $p < 0.05$ vs Vehicle at the same time point according to Student's *t*-test. (G) Survival rate after injection of 0.2 mg/L E171. Median survival of vehicle = 14 days and E171 = 12 days. Curve comparison: $p = 0.487$ Log-rank analysis and $p = 0.282$ Gehan-Breslow-Wilcoxon test.

3.2. Toxicokinetic studies in mice

Although when ingested E171 is poorly systemically available, a small percentage of TiO₂ NPs can circulate in the bloodstream for a long time due to their long half-lives, from 28 up to 650 days (EFSA, 2021). To investigate whether serum affected the colloidal properties of E171, TEM analysis was done on the material suspended in water or murine serum and incubated for 1, 4 and 24 hours at 37°C. E171 particles in water were homogeneously distributed at all time points considered, and their tendency to remain separate enabled us to observe their spherical shape of different sizes for a large number of TiO₂ NPs (Fig 2A). However, when E171 was suspended in serum, the particles formed large compact clusters (0.5-1 μm) regardless of the incubation time, making it almost impossible to distinguish the shape of single NPs (Fig. 2B-D). These findings indicate that serum affects the morphological characteristics of E171 and promotes the clustering of TiO₂ particles, influencing their biodistribution *in vivo*.

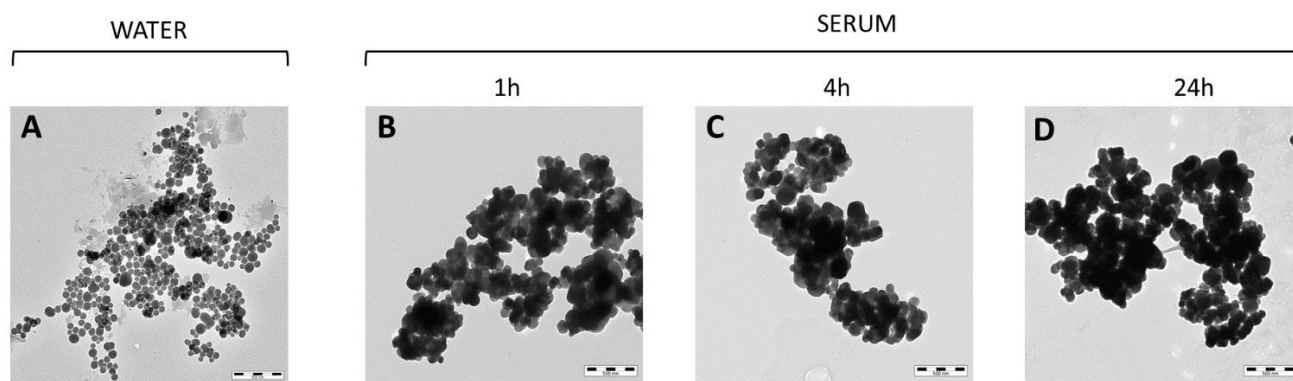


Figure 2. Effect of serum on E171 particles. Representative TEM images of E171 incubated in (A) water or (B, C, D) murine serum for 1, 4 and 24 hours. Scale bars=500 nm.

Healthy mice were then intravenously treated with E171 (6 mg/kg b.w.) and the elemental Ti concentration (originating from the TiO₂ NPs) in blood (Fig. 3A) and in organs (Fig. 3B) was determined by ICP-MS at from 1 h up to one week after injection. Ti blood concentrations peaked one hour after injection, representing about 1% of the injected dose (ID), decreased by ~60% by 4 hours and remained very low for up to 168 hours, suggesting that circulating E171 NPs rapidly penetrated various organs or was cleared quickly. The low TiO₂ concentrations (in terms of detected Ti), as a percentage of the ID, in liver, spleen and kidneys seem to confirm the hypothesis of rapid clearance and poor filtration by liver and spleen macrophages, and the lack of accumulation in kidneys at 1 and 24 hours argues against this elimination being by renal filtration. As expected, in the brain there was a drastic decrease in TiO₂ concentrations (in terms of detected Ti) from 1 to 24 hours after injection. It is therefore likely that the amount measured at 1 h was almost entirely due to blood in the cerebral vessels. In contrast, the pattern of Ti accumulation in the lungs was surprisingly higher than in the other organs and increased over time (Fig. 3B).

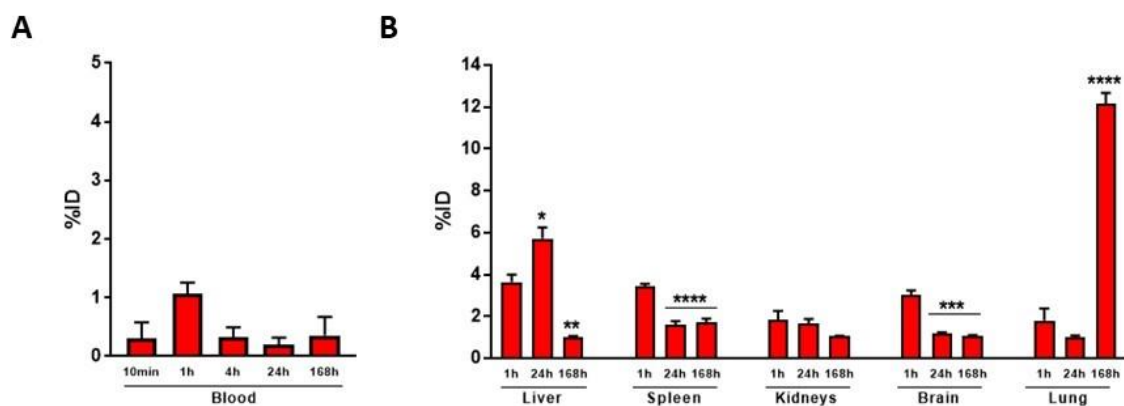


Figure 3. Titanium content in organs. Elemental titanium in (A) blood, and (B) liver, spleen, kidneys, brain and lungs of mice intravenously treated with 6 mg/kg b.w. E171. Ti content was determined by inductively coupled plasma mass spectrometry (ICP-MS) on tissues collected at different times after the E171. Data are percentages of the injected dose (% ID). Each data point represents the mean \pm S.E.M. (N=3). * $p < 0.05$, ** $p < 0.005$, *** $p < 0.0005$, and **** $p < 0.0001$ vs 1 hour, according to one-way ANOVA and Bonferroni *post hoc* tests.

We next wanted to define the toxicity profile of E171 on circulating hematopoietic cells. A complete blood count was obtained 12 hours after vehicle or E171 injection. Complete blood cell analysis showed that the total numbers of circulating WBC, lymphocytes and neutrophils were not affected by E171 administration (Fig. 4A-C), whereas the number of monocytes increased significantly (Fig. 4D). Monocytes are the circulating myeloid cells that, once recruited to tissues and organs such as the liver, differentiate into macrophages and are devoted to the elimination of many exogenous molecules by phagocytosis, including E171 (Medina-Reyes et al., 2020). Therefore, it is possible that circulating monocytes were rapidly required to remove TiO_2 particles from the bloodstream and other organs. Importantly, there was no difference in circulating platelets (Fig. 4E), suggesting that E171 did not affect platelet activation and function.

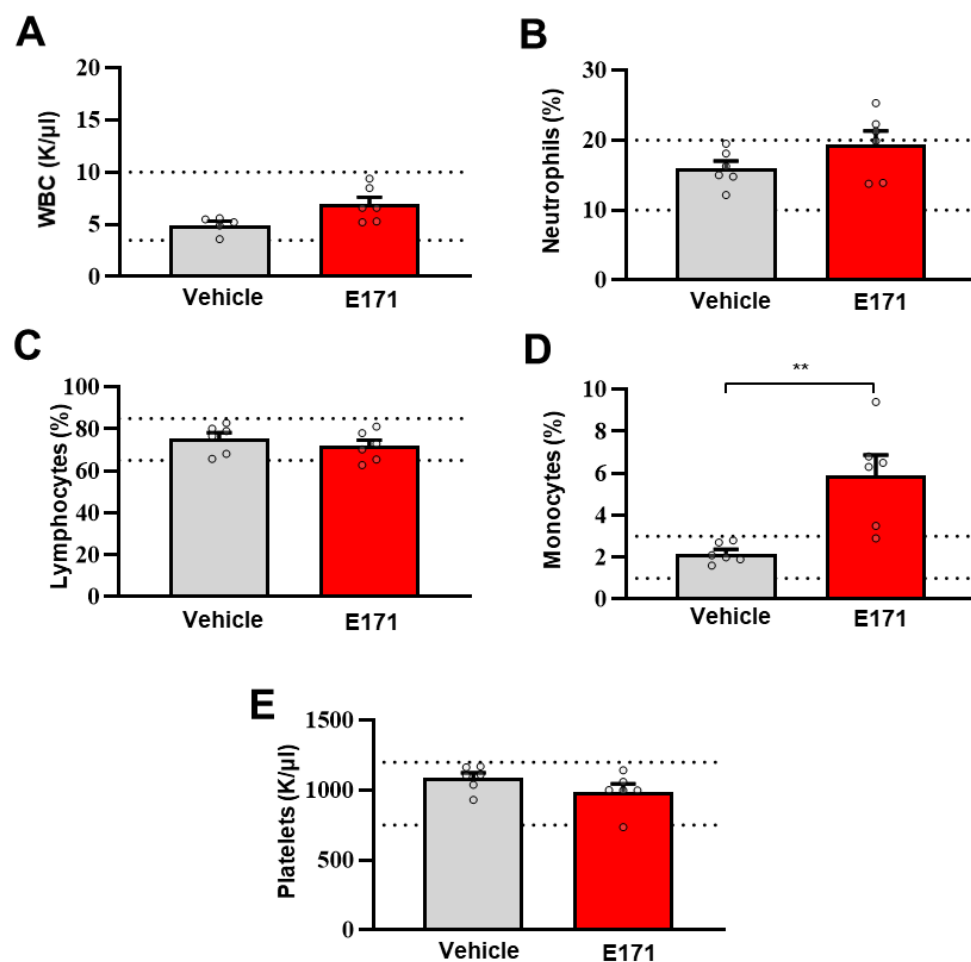


Figure 4. Effect of E171 on complete blood cell count. (A) Total white blood cells (WBC), (B) neutrophils, (C) lymphocytes, (D) monocytes and (E) platelets of mice were measured 12 hours after the intravenous injection of E171. Control mice were treated with vehicle alone (Vehicle). The dotted lines indicate the upper and lower normal value for each variable (4-10 K/uL for WBC, 65-87% for lymphocytes, 10-20% for neutrophils, 1-3% for monocytes and 750-1250 K/uL for platelets). Data are mean \pm S.E.M. (N=6). **p < 0.005 *vs* vehicle mice, two-tailed Mann-Whitney test.

Although the level of Ti originating from the TiO₂ NPs in the blood, liver, kidneys, spleen, and brain was indicative of low accumulation, we examined whether it caused signs of toxicity. Serum levels of sALT (Fig. 5A), a hepatocellular enzyme released into the bloodstream after hepatocellular cell death (Talamini et al., 2019), sAST and LDH (Fig. 5B, C), released in the circulation after cell death in the liver and other tissues such as blood cells, kidneys, brain and lungs (Chan et al., 2013), were measured as markers of tissue damage. No significantly different levels of sALT, sAST and LDH were seen in animals treated with E171 compared to vehicle-treated mice, indicating that Ti accumulation in organs did not induce toxicity.

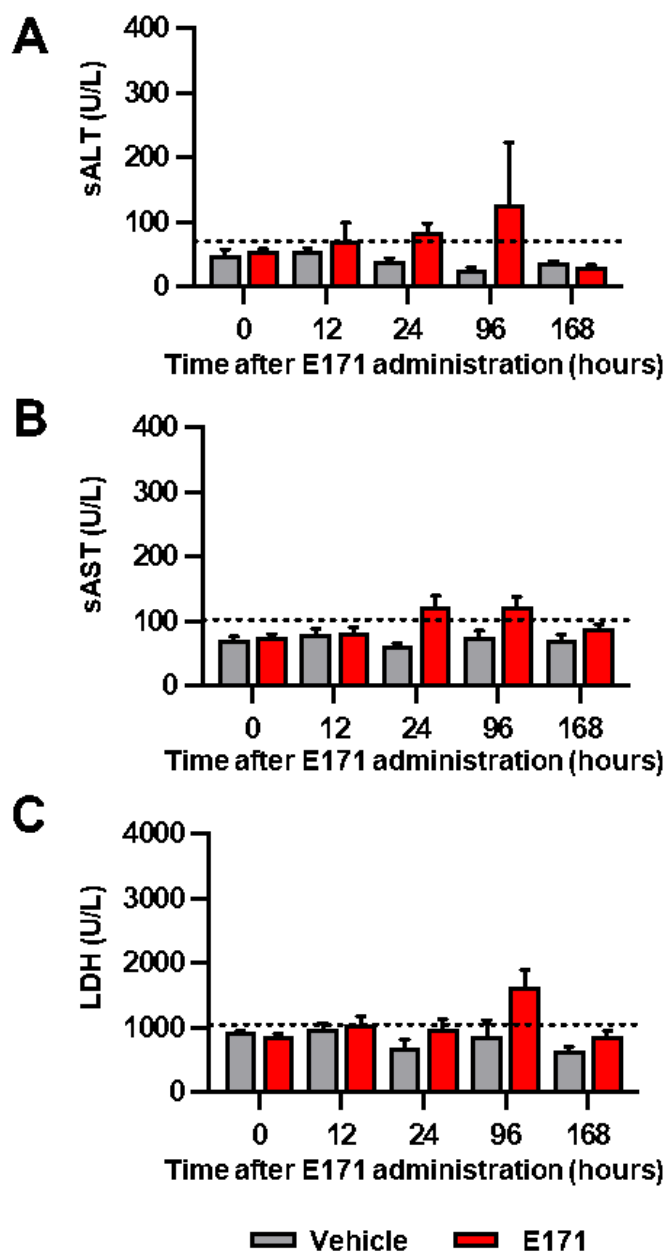


Figure 5. Effect of E171 on serum biochemical parameters. (A) sALT, (B) sAST and (C) sLDH activity were measured in serum of mice before and different times after the injection of E171 or vehicle. The dotted lines indicate the upper normal value for each variable (43 U/L for sALT, 104 U/L for sAST, and 1100 U/L for LDH). Data are expressed as Units/liter (U/L). Values are the mean \pm S.E.M. (N=6). No significant difference was found between E171-treated mice *vs.* Vehicle mice, two-way ANOVA and Bonferroni *post hoc* test.

To gain information on this hypothesis, groups of E171 or vehicle-treated mice were euthanized 1, 24, and 168 hours after injection for pathological evaluation of liver and lungs. Initially, livers were examined either by histopathological analysis (H&E staining) or by immunostaining with the F4/80 antibody, a marker directed against tissue resident macrophages or monocytes. As expected, there were no marked signs of inflammation, steatosis, necrosis, or other tissue alterations in specific pathogen-free immunocompetent mice given vehicle. The E171-treated mice had small microgranulomas already after one hour (Fig. 6, red dashed lines). These changes became less pronounced 24 hours after E171 and had completely disappeared 6 days later. These results suggested that TiO₂ NPs can accumulate, albeit in small amounts, in the liver parenchyma, close to F4/80⁺ resident intravascular Kupffer cells and/or myeloid cells recruited from the circulation (Fig. 4D). The

increased myeloid population in the liver formed transient microgranulomas to remove NPs, similarly to what has been reported for mice given TiO₂ NPs and E171 orally (Heringa et al., 2016) (Talamini et al., 2019). The ICP-MS data in Fig. 3 indicated that after the E171 injection, the level of Ti in the liver peaked within the first 24 hours and returned to the basal level after 7 days. This suggests that TiO₂ NPs accumulating in the liver can be efficiently cleared, causing only low and transient toxicity, with no signs of chronic hepatic disease (see also Fig. 5).

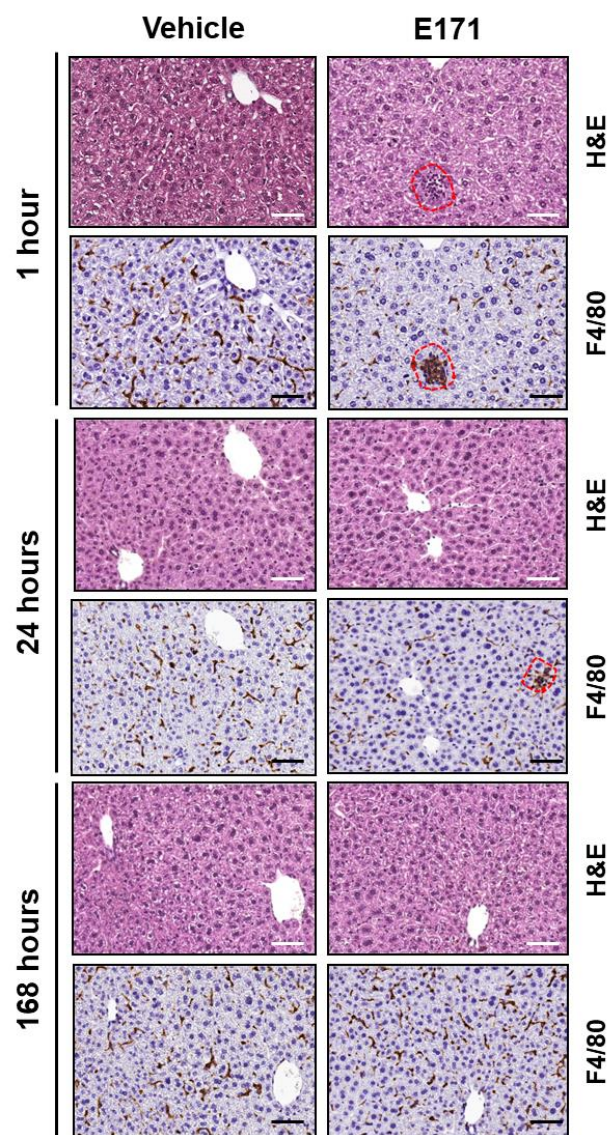


Figure 6. Pathological examination of livers of mice treated with E171. Representative images of liver hematoxylin-eosin (H&E) and F4/80 immunostaining of mice injected with vehicle or E171 and euthanized 1, 24 and 168 hours after injection. Small microgranulomas were detected 1 and 24 hours but not at 168 hours after E171, and were indicative of low-grade transient inflammation due to E171.

We then determined the level of toxicity induced by E171 in the lungs which, from ICP-MS analysis, were the organs with the highest accumulation of Ti, at least 7 days after the injection. The lungs of the E171-injected mice euthanized after injection 1, 24, and 168 hours were examined by immunostaining with the F4/80 antibody to determine the accumulation of macrophages and to verify whether Ti accumulation can lead to direct modification of the parenchyma. Similar to what was seen in the liver, interstitial inflammation with recruitment of F4/80⁺ cells was weak at the first time points and increased with Ti accumulation. While one hour after E171 injection there was no evidence of lung

parenchyma F4/80 staining, at 24 hours morphological alteration in lung tissue was observed, which was further enhanced in sections from animals euthanized 168 hours after injection (Fig. 7A). At this time point, the lungs of E171-treated mice displayed significantly more interstitial immunoreactivity in the alveoli than those injected with vehicle (Fig. 7B). This progressive change was very likely due to the increasing TiO₂ accumulation in the lungs (see Fig. 3).

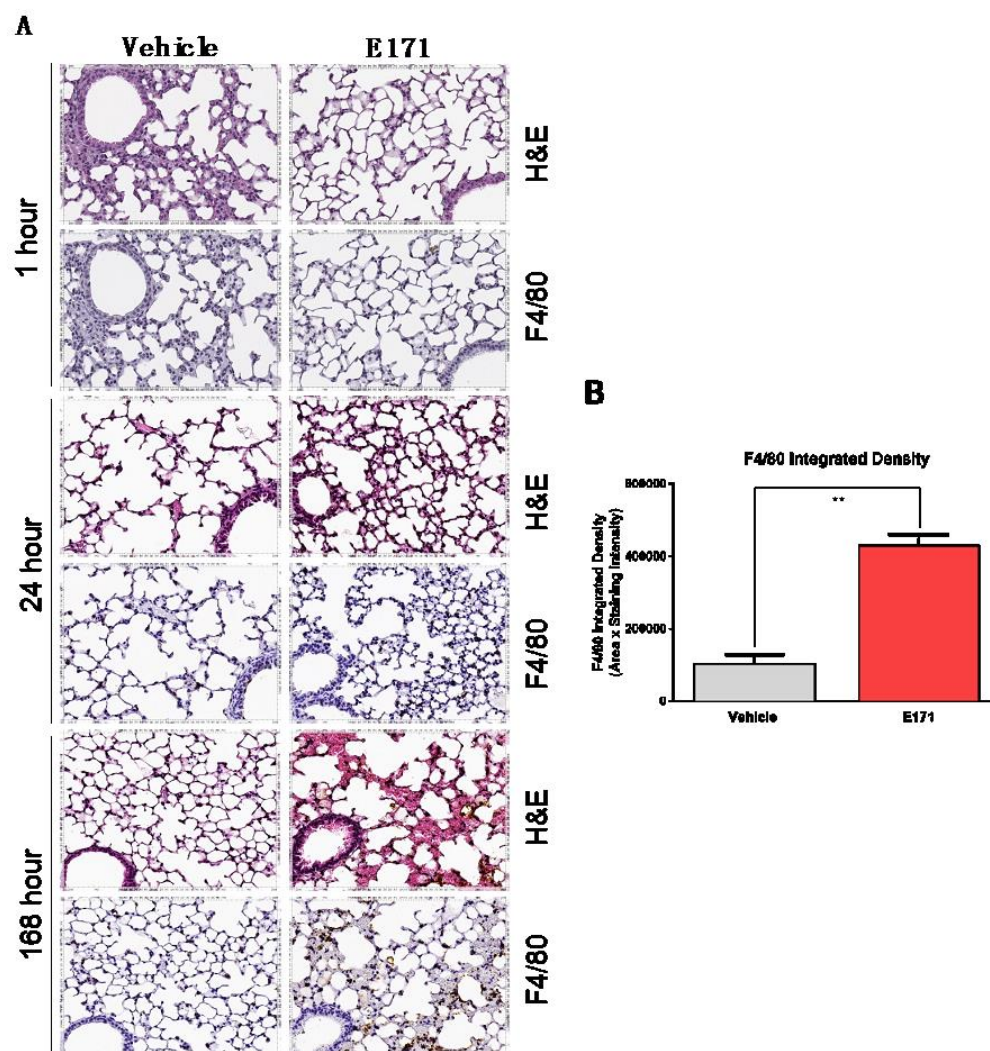


Figure 7. Pathological examination of the lungs of E171-injected mice. (A) Representative images of F4/80 immunostaining of lung sections from mice treated with vehicle or E171 and euthanized 1, 24, and 168 hours after injection. (B) F4/80 immunoreactivity of slices from mice euthanized 168 hours after treatment. Values are mean \pm S.E.M. (N= 5). **p<0.01 vs. vehicle, unpaired Student's t-test.

4. Discussion

TiO₂ is a nanomaterial used in many products, that have potential effects through various routes of entry (skin, respiratory tract, ingestion) (Gui et al., 2011). We focused on the potential impact of the widely utilized food-grade form of TiO₂, E171, in invertebrate and vertebrate animals estimating parameters such as penetration, accumulation, and toxicity.

Like other types of TiO₂ NPs (Iannarelli et al., 2016) (Ma et al., 2019) (Hu et al., 2020), E171 can be absorbed by *C. elegans*, passing the biological barriers and exerting acute toxicological effects. Of particular concern is its effects on the reproduction and development of worms, which confirms the ability of TiO₂ NPs to cause a damage that can be transmitted from one generation to another. Toxicity scores in *C. elegans* have repeatedly proved

predictive of toxic parameters in rodents (Hunt, 2017) indicating that, although nematodes alone cannot replace experiments in mammals for hazard identification, they can offer important translational information.

Recent studies have found evidence of downstream events outside the gastrointestinal tract. These share the mechanism of absorption through capillaries and vessels and entry into the circulatory system with subsequent systemic diffusion (Wang et al., 2007). Therefore, in the present study we investigated the potential effects of single systemic over-exposure to E171 in immunocompetent healthy mice. In our previous study (Talamini et al., 2019) ICP-MS showed the liver was poorly able to retain E171. Even in this more favorable condition, however, where NPs flow directly into the bloodstream, the amount of hepatic TiO₂ was several times lower than in our previous studies and, more generally, than in the comprehensive characterization of nanogold behavior recently published by Tsoi et al. (Tsoi et al., 2016). This confirms the strong tropism of hard materials towards the liver and their ability to be internalized in cells of the reticular endothelial system (Talamini et al., 2017) (Li and Lane, 2018).

Surprisingly, compared to gold NPs kinetics, the ICP-MS measurements showed a relatively low uptake of TiO₂ NPs from the liver and complete disappearance from 1 to 7 days. This transient phenomenon seems to rely on efficient uptake by liver macrophages. However, despite this minimal accumulation, weak, transient, but readily detectable histological changes were observed in the liver parenchyma as early as one hour after E171.

The lower absorptive capacity of the liver components might indicate a greater filtering action of the spleen or rapid clearance and excretion by the kidneys, which would support the safe use of these materials. However, renal levels of TiO₂ as early as the first hour did not seem to indicate that the NPs were rapidly excreted in the urine, and the very moderate accumulation in spleen indicates low uptake by red pulp macrophages (Pelaz et al., 2017).

Unexpectedly, there was a progressive, increasing lung accumulation of TiO₂ in mice given a single intravenous dose of E171. The lack of further time points makes it difficult to establish whether day 7 is the peak of lung accumulation. However, this behavior is strange, but it is obvious that such long duration cannot be explained by the hypothesis that circulating NPs remain in the bloodstream for 7 days, given the ICP-MS results in plasma. Therefore, it is possible that they somehow remain trapped in the endothelium where NPs were gradually released and taken up by the lungs from day 1 to day 7, or else they were engulfed by circulating monocytes, as shown by the significantly higher numbers of monocytes in the blood of animals treated with E171 as early as 12 hours after treatment.

A possible explanation why NPs in the 35 to 150 nm range are taken up by lungs rather than by macrophages residing in the spleen and liver might be the irrelatively rapid aggregation in the circulation (Liao et al., 2013). Size plays a role in organo-specific bio-distribution of circulating particles. In general, spherical or spheroidal particles smaller than 10 nm are efficiently retained by renal tubules and then excreted in the urine, while particles from 500 nm to 1 μ m remain trapped in the lungs (Wei et al., 2012). The others generally accumulate efficiently in the liver and spleen, at different rates depending on surface area, charge, and coating. This assumption holds for stable NPs specifically synthesized and coated using surfactants to maintain a high degree of monodispersity in biological fluids. This is not the case for E171, where there is no precise surface functionalization and they are not colloidal stable in serum-containing medium (Fig. 2). It is therefore likely that aggregates larger than 500 nm form gradually and that this "size transformation" may lead to concomitant release from the liver but increased in accumulation in the lungs. The lack of colloidal stability after entering the bloodstream seems to be experimentally confirmed by the TEM analyses of E171 after serum incubation. Our results point to an increase of diameter of the single particles and lack of homogeneity of both the shape and outer surface of NPs exposed to serum proteins, which eventually leads to progressive aggregation, resulting in spurious microparticles (Bischoff et al., 2021).

It is therefore possible that this unexpected increase in lung Ti levels is due to the formation of NP microaggregates rather than to an active mechanism of endothelial transcytosis or macrophage uptake. Alternatively, it is tempting to speculate that Kupffer cells in the liver and recruited monocytes/macrophages, after a first wave of uptake in the liver, die and release TiO₂ into the circulation in small amounts that aggregate secondarily in the lungs, as indicated by the different kinetics of accumulation in these two organs. Consistently with this hypothesis, our recent study (Talamini et al., 2017) demonstrated the strong influence of geometry on the biodistribution of gold NPs. Interestingly, neither size nor shape resulted in substantial toxicity in treated mice. When NPs agglomerate, their initial size and shape loses importance (Tay et al., 2014). This is an extremely important indication that it is not just how much material is accumulated, but where it accumulates in the parenchyma. The evidence of specific, well-limited foci of inflammation in the liver, despite such a small accumulation, strongly suggests the presence of microinfarcts in the sinusoids due to clogging with aggregated E171 NPs. The efficiency of the immune system in clearing the debris of dying cells along with the entrapped E171 and the transient effect of the process is clear. This may be responsible for both the disappearance of titanium from day 1 to day 7 and the absence of infiltrates in the liver at this last.

This study offers further information of the potential risk of exposure to TiO₂ NPs in food products. Expanding on our recent work in mice (Talamini et al., 2019), we examined the effects of acute exposure to the nematode *C. elegans* and found that E171 activates important pathological mechanisms despite the difference in route of administration and the morpho-functional differences between the two species. Therefore, this study not only reinforces the reliability of preliminary tests with *C. elegans* for bio-nano interaction studies but also give us the chance to focus on the fate of food-grade TiO₂ NPs after internal absorption in mice.

The unexpected tropism towards the lungs, not without histopathological changes, in animals treated systemically with E171 has a plausible explanation in the progressive loss of colloidal stability leading to aggregation and preventing penetration through the hepatic sinusoids and entrapment of micrometric particles in the pulmonary microcirculation. Although much more research is needed, selecting specific modes of administration and chronic exposure, this analysis offers useful insights for the evaluation of physicochemical parameters of NPs. The results support the recent European decision to ban E171 and limit the use of TiO₂ NPs to avoid any impact on human and environmental health.

Funding: Parts of this research was supported by the Cluster of Excellence 'Advanced Imaging of Matter' of the Deutsche Forschungsgemeinschaft (DFG), grant number EXC 2056, project ID 390715994 (W.J.P.), and by the Italian Association for Cancer Research (AIRC), grant numbers 22820 and 22737 (G.S.).

Acknowledgements: *C. elegans* and OP50 *E. coli* were provided by the GCG, which is funded by NIH Office Research Infrastructure Programs ([P40 OD010440](#)).

Author Contributions: Conceptualization, F.F., L.D. and P.B.; Methodology, G.S., F.F., M.B.V., L.T., A.C., L.M.F., N.L.T., I.C. and W.J.P.; Formal Analysis, G.S., M.B.V. and L.D.; Investigation, G.S., F.F., M.B.V., L.T., A.C., L.M.F., N.L.T., I.C. and W.J.P.; Writing – Original Draft Preparation, G.S., F.F., J.F.A., L.D. and P.B.; Writing – Review & Editing, G.S., F.F., M.S., L.D. and P.B.; Supervision, F.F., M.S., L.D. and P.B.; Funding Acquisition, G.S. and W.J.P.

Data Availability Statement: The data presented in this study are available on request from the corresponding author.

Conflicts of Interest: The authors declare no conflict of interest.

References

1. Chow, J. C., Watson, J. G., Lowenthal, D. H., Chen, L. A. and Magliano, K. L. Particulate carbon measurements in California's San Joaquin Valley. *Chemosphere*, **2006**, 62 (3): 337-48; DOI:10.1016/j.chemosphere.2005.04.094.
2. Pope, C. A. 3rd, Burnett, R. T., Thurston, G. D., Thun, M. J., Calle, E. E., Krewski, D., Godleski, J. J. Cardiovascular mortality and long-term exposure to particulate air pollution: epidemiological evidence of general pathophysiological pathways of disease. *Circulation*, **2014**, 109 (1): 71-7; DOI:10.1161/01.CIR.0000108927.80044.7F.
3. Tucci, P., Porta, G., Agostini, M., Dinsdale, D., Iavicoli, I., Cain, K., Finazzi-Agró, A., Melino, G., Willis, A. Metabolic effects of TiO₂ nanoparticles, a common component of sunscreens and cosmetics, on human keratinocytes. *Cell Death Dis*, **2013**, 4 (3): e549; DOI:10.1038/cddis.2013.76.
4. Trouiller, B., Reliene, R., Westbrook, A., Solaimani, P., Schiestl, R. H. Titanium dioxide nanoparticles induce DNA damage and genetic instability in vivo in mice. *Cancer Res*, **2009**, 69 (22): 8784-9; DOI:10.1158/0008-5472.CAN-09-2496.
5. Musial, J., Krakowiak, R., Mlynarczyk, D. T., Goslinski, T., Stanisz, B. J. Titanium Dioxide Nanoparticles in Food and Personal Care Products—What Do We Know about Their Safety? *Nanomaterials*, **2020**, 10 (6): 1110; DOI:10.3390/nano10061110.
6. Titanium Dioxide Market Trends Analysis Report, 2021-2028. <https://www.grandviewresearch.com/industry-analysis/titanium-dioxide-industry> (accessed on 22 October 2021).
7. Kakihana, M., Kobayashi, M., Tomita, K. and Petrykin, V. Application of Water-Soluble Titanium Complexes as Precursors for Synthesis of Titanium-Containing Oxides via Aqueous Solution Processes. *Bull. Chem. Soc. Jpn.*, **2010**, 11, 1285–1308; DOI:10.1246/bcsj.20100103.
8. IARC. IARC Working Group on the Evaluation of Carcinogenic Risks to Humans: Polychlorinated Dibenzo-Para-Dioxins and Polychlorinated Dibenzofurans. *IARC Monogr Eval Carcinog Risks Hum*, **1997**, 69, 1–631.
9. Riebeling, C., Haase, A., Tralau, T. and Luch, A. Substance classification of titanium dioxide illustrates limitations of EU legislation. *Nat Food*, **2020**, 1, 523–525; DOI:10.1038/s43016-020-00149-w.
10. NIOSH, National Institute for Occupational Safety and Health. <https://www.cdc.gov/niosh/index.htm> (accessed 25 October 2021).
11. NEDO, New Energy and Industrial Technology Development Organization. <https://www.nedo.go.jp> (accessed 25 October 2021).
12. Scientific Committee on Consumer Safety SCCS OPINION on Titanium dioxide (TiO₂) used in cosmetic products that lead to exposure by inhalation. *Annex VI, Cosmetics Regulation 1223/2009*, SCCS/1617/20 Final opinion.
13. CFR - Code of Federal Regulations Title 21. <https://www.accessdata.fda.gov/scripts/cdrh/cfdocs/cfcfr/cfrsearch.cfm?fr=73.575> (accessed 25 October 2021).
14. EFSA. Re-evaluation of titanium dioxide (E171) as a food additive | Autorità europea per la sicurezza alimentare. *EFSA Journal*, **2016**, 14 (9): e04545. <https://www.efsa.europa.eu/en/efsajournal/pub/4545> (accessed 25 October 2022).

15. EFSA. Safety assessment of titanium dioxide (E171) as a food additive." *EFSA Journal*, **2021**.
<https://doi.org/10.2903/j.efsa.2021.6585> (accessed 25 October 2021).
16. EFSA. Scientific Panel on Food Additives and Nutrient Sources added to Food (ANS).
<https://www.efsa.europa.eu/sites/default/files/event/180515-m.pdf> (accessed 25 October 2021).
17. Weir, A., Westerhoff, P., Fabricius, L., Hristovski, K. and von Goetz, N. Titanium dioxide nanoparticles in food and personal care products. *Environ Sci Technol*, **2012**, *46*, 2242–2250; DOI:10.1021/es204168d.
18. Peters, R. J. B., Bommel, G., Herrera-Rivera, Z., Helsper, H. P. F. G., Marvin, H. J. P., Weigel, S., Tromp, P. C., Oomen, A. G., Rietveld, A. G. and Bouwmeester, H. Characterization of titanium dioxide nanoparticles in food products: analytical methods to define nanoparticles. *J Agric Food Chem*, **2014**, *62*, 6285–6293; DOI:10.1021/jf5011885.
19. Dufefoi, W., Terrisse, H., Richard-Plouet, M., Gautron, E., Popa, F., Humbert, B. and Ropers, M. Criteria to define a more relevant reference sample of titanium dioxide in the context of food: a multiscale approach. *Food Addit Contam Part A Chem Anal Control Expo Risk Assess*, **2017**, *34*, 653–665; DOI:10.1080/19440049.2017.1284346.
20. Fiordaliso, F., Foray, C., Salio, M., Salmona, M. and Diomede, L. Realistic Evaluation of Titanium Dioxide Nanoparticle Exposure in Chewing Gum. *J. Agric. Food Chem.*, **2018**, *66*, 6860–6868; DOI:10.1021/acs.jafc.8b00747.
21. ISO/TS 80004-1:2015. Commission Recommendation of 18 October 2011 on the definition of nanomaterialText with EEA relevance. 3.: ISO
<https://www.iso.org/cms/render/live/en/sites/isoorg/contents/data/standard/06/80/68058.html> (accessed 25 October 2021).
22. ISO/TS 80004-2:2015. Commission Recommendation of 18 October 2011 on the definition of nanomaterialText with EEA relevance. 3.: ISO
<https://www.iso.org/cms/render/live/en/sites/isoorg/contents/data/standard/05/44/54440.html> (accessed 25 October 2021).
23. Fiordaliso F., Bigini P., Salmona M. and Diomede L. Toxicological impact of titanium dioxide nanoparticles and food-grade titanium dioxide (E171) on human and environmental health. *Environ. Sci.: Nano.*, **2022**;
DOI:10.1039/D1EN00833A.
24. Shi, H., Magaye, R., Castranova, V. and Zhao, J. Titanium dioxide nanoparticles: a review of current toxicological data. *Part Fibre Toxicol*, **2013**, *10*, 15; DOI:10.1186/1743-8977-10-15.
25. Zhang, R., Bai, Y., Zhang, B., Chen, L. and Yan, B. The potential health risk of titania nanoparticles. *Journal of Hazardous Materials*, **2012**, 211–212, 404–413; DOI:10.1016/j.jhazmat.2011.11.022.
26. Guillard, A., Gaultier, E., Cartier, C., et al. Basal Ti level in the human placenta and meconium and evidence of a materno-foetal transfer of food-grade TiO₂ nanoparticles in an ex vivo placental perfusion model. *Particle and Fibre Toxicology*, **2020**, *17*, 51; DOI:10.1186/s12989-020-00381-z.
27. Rollerova, E., Tulinska, J., Liskova, A., Kuricova, M., Kovriznych, J., Mlynarcikova, A., Kiss, A. and Scsukova, S. Titanium dioxide nanoparticles: some aspects of toxicity/focus on the development. *Endocr Regul*, **2015**, *49*, 97-112; DOI:10.4149/endo_2015_02_97.
28. Iannarelli, L., Giovannozzi, A. M., Morelli, F., Viscotti, F., Bigini, P., Maurino, V., Spoto, G., Martra, G., Ortel, E., Hodoroaba, V., Rossi, A. M. and Diomede, L. Shape Engineered TiO₂ Nanoparticles in *Caenorhabditis elegans*: a Raman Imaging Based Approach to Assist Tissue-Specific Toxicological Studies. *RSC Adv.*, **2016**, *6*;
DOI:10.1039/C6RA09686G.
29. Hunt, P. R. The *C. elegans* model in toxicity testing. *J. Appl. Toxicol.*, **2017**, *37*: 50-59; DOI:10.1002/jat.3357.

30. Frézal, L. and Félix, M. The natural history of model organisms: *C. elegans* outside the petri dish. *eLife*, **2015**, 4: e05849; DOI:10.7554/eLife.05849.
31. Talamini, L., Gimondi, S., Violatto, M. B., Fiordaliso, F., Pedica, F., Tran, N. L., Sitia, G., Aureli, F., Raggi, A., Nelissen, I., Cubadda, F., Bigini, P. and Diomede, L. Repeated administration of the food additive E171 to mice results in accumulation in intestine and liver and promotes an inflammatory status. *Nanotoxicology*, **2019**, 13 (8): 1087-1101; DOI:10.1080/17435390.2019.1640910.
32. Bischoff, N. S., Kok, T. M., Sijm, D. T. H. M., van Breda, S. G., Briedé, J. J., Castenmiller, J. J. M., Opperhuizen, A., Chirino, Y. I., Dirven, H., Gott, D., Houdeau, E., Oomen, A. G., Poulsen, M., Rogler, G. and van Loveren, H. P. Possible Adverse Effects of Food Additive E171 (Titanium Dioxide) Related to Particle Specific Human Toxicity, Including the Immune System. *Int. J. Mol. Sci*, **2021**, 22, 207; DOI:10.3390/ijms22010207.
33. Kreyling, W., Abdelmonem, A., Ali, Z. et al. In vivo integrity of polymer-coated gold nanoparticles. *Nature Nanotechnology*, **2015**, 10, 619–623; DOI:10.1038/nnano.2015.111.
34. Catarinella, M., Monestiroli, A., Escobar, G., Fiocchi, A., Tran, N. L., Aiolfi, R., Marra, P., Esposito, A., Cipriani, F., Aldrighetti, L., Iannaccone, M., Naldini, L., Guidotti, L. G. and Sitia, G. IFN α gene/cell therapy curbs colorectal cancer colonization of the liver by acting on the hepatic microenvironment. *EMBO Mol Med*, **2016**, 8 (2): 155-70; DOI:10.15252/emmm.201505395.
35. Medina-Reyes, E. I., Rodríguez-Ibarra, C., Déciga-Alcaraz, A., Díaz-Urbina, D., Chirino, Y. I. and Pedraza-Chaverri, J. Food additives containing nanoparticles induce gastrototoxicity, hepatotoxicity and alterations in animal behavior: The unknown role of oxidative stress. *Food and Chemical Toxicology*, **2020**, 146, 111814; DOI:10.1016/j.fct.2020.111814.
36. Chan, F. K., Moriwaki, K. and Rosa, M. J. Detection of Necrosis by Release of Lactate Dehydrogenase (LDH) Activity. *Methods Mol Biol*, **2013**, 979: 65–70; DOI:10.1007/978-1-62703-290-2_7.
37. Heringa, M. B., Geraets, L., Eijkeren, J. C. H., Vandebriel, R. J., Jong, W. H. and Oomen, A. G. Risk assessment of titanium dioxide nanoparticles via oral exposure, including toxicokinetic considerations. *Nanotoxicology*, **2016**, 10 (10): 1515-1525; DOI:10.1080/17435390.2016.1238113.
38. Gui, S., Zhang, Z., Zheng, L., Cui, Y., Liu, X., Li, N., Sang, X., Sun, Q., Gao, G., Cheng, Z., Cheng, J., Wang, L., Tang, M., and Hong, F. Molecular mechanism of kidney injury of mice caused by exposure to titanium dioxide nanoparticles. *J Hazard Mater*, **2011**, 195: 365-70; DOI:10.1016/j.jhazmat.2011.08.055.
39. Ma, H., Lenz, K. A., Gao, X., Li, S. and Wallis, L. K. Comparative toxicity of a food additive TiO₂, a bulk TiO₂, and a nano-sized P25 to a model organism the nematode *C. elegans*. *Environ Sci Pollut Res Int*, **2019**, 26 (4): 3556-3568 ; DOI:10.1007/s11356-018-3810-4.
40. Hu, C., Hou, J., Zhu, Y. and Lin, D. Multigenerational exposure to TiO₂ nanoparticles in soil stimulates stress resistance and longevity of survived *C. elegans* via activating insulin/IGF-like signaling. *Environ Pollut*, **2020**, 263 (Pt A): 114376 ; DOI:10.1016/j.envpol.2020.114376.
41. Wang, J., Zhou, G., Chen, C., Yu, H., Wang, T., Ma, Y., Jia, G., Gao, Y., Li, B., Sun, J., Li, Y., Jiao, F., Zhao, Y. and Chai, Z. Acute toxicity and biodistribution of different sized titanium dioxide particles in mice after oral administration. *Toxicol Lett*, **2007**, 168 (2): 176-85; DOI:10.1016/j.toxlet.2006.12.001.
42. Tsoi, K., MacParland, S., Ma, XZ. et al. Mechanism of hard-nanomaterial clearance by the liver. *Nature Mater*, **2016**, 15, 1212–1221; DOI:10.1038/nmat4718.
43. Talamini, L., Violatto, M. B., Cai, Q., Monopoli, M. P., Kantner, K., Krpetić, Ž., Perez-Potti, A., Cookman, J., Garry, D., P Silveira, C., Boselli, L., Pelaz, B., Serchi, T., Cambier, S., Gutleb, A. C., Feliu, N., Yan, Y., Salmona, M., Parak, W. J., Dawson, K. A., et al. Influence of Size and Shape on the Anatomical Distribution of Endotoxin-Free Gold Nanoparticles. *ACS Nano*, **2017**, 11(6): 5519-5529; DOI:10.1021/acsnano.7b00497.

44. Li, B. and Lane, L. A. Probing the biological obstacles of nanomedicine with gold nanoparticles. *WIREs Nanomed Nanobiotechnol*, **2018**, *11*: e1542; DOI:10.1002/wnan.1542.
45. Pelaz, B., Alexiou, C., Alvarez-Puebla, R. A., Alves, F., Andrews, A. M., Ashraf, S., Balogh, L. P., Ballerini, L., Bestetti, A., Brendel, C., Bosi, S., Carril, M., Chan, W. C., Chen, C., Chen, X., Chen, X., Cheng, Z., Cui, D., Du, J., Dullin, C., et al. Diverse Applications of Nanomedicine. *ACS Nano*, **2017**, *11*, 3, 2313–2381; DOI:10.1021/acsnano.6b06040.
46. Liao, W., Li, H., Chang, M., Tang, A. C. L., Hoffman, A. S. and Hsieh, P. C. H. Comprehensive characterizations of nanoparticle biodistribution following systemic injection in mice. *Nanoscale*, **2013**, *5*, 11079-11086; DOI:10.1039/C3NR03954D.
47. Wei, Z., Chen, L., Thompson, D. M. and Montoya, L. D. Effect of particle size on in vitro cytotoxicity of titania and alumina nanoparticles. *Journal of Experimental Science*, **2012**, *6*, 625-638; DOI:10.1080/17458080.2012.683534.
48. Tay, C. Y., Setyawati, M. I., Xie, J., Parak, W. J. and Leong, D. T. Back to Basics: Exploiting the Innate Physico-chemical Characteristics of Nanomaterials for Biomedical Applications. *Advanced Functional Materials*, **2014**, *24*, 5936–5955; DOI:10.1002/adfm.201401664.